ChemComm
Chemical Communications

Accepted Manuscript

This article can be cited before page numbers have been issued, to do this please use: F. Geng, D. Wang, L. Feng, G. Li and M. Xu, *Chem. Commun.*, 2020, DOI: 10.1039/D0CC03669B.

ROYAL SOCIETY OF CHEMISTRY

rsc.li/chemcomm

View Article Online
DOI: 10.1039/D0CC03669B

COMMUNICATION

Improved structure-switch aptamer based fluorescent Pb^{2+} biosensor utilizing binding induced quenching of AMT to G-quadruplex

Received 00th January 20xx,
Accepted 00th January 20xx

DOI: 10.1039/x0xx00000x

Fenghua Geng, [a,b,†] Dandan Wang,[c,†] Li Feng*[a], Guixin Li [c] and Maotian Xu *[b]

Improved aptamer based fluorescent Pb^{2+} biosensor utilizing binding induced quenching of AMT to G-quadruplex has been rationally designed with the LOD of 3.6 nM. The utility of the developed biosensor was demonstrated by the successful detection of in real complex clinic samples with satisfactory recovery and good reproducibility.

With the increasing use of lead (Pb^{2+}) containing petroleum and chemical products (such as gasoline, batteries, plastics, electronic products and chemical coatings, etc.), as a common toxic heavy metal ion pollutant, Pb^{2+} ions can be widely entered in a variety of ways in environment, not only directly cause serious pollution to the atmosphere, water, soil, but also indirectly affect the nerves, hematopoietic, digestion, kidneys, heart through the food chain after entering the human body because of its strong accumulation, especially affect children's intelligence and growth. [1] Therefore, rapid and sensitive detection of trace Pb^{2+} is of vital importance in effectively preventing Pb^{2+} pollution and diagnosing related diseases. Established traditional methods for Pb^{2+} detection include atomic absorption / emission spectroscopy [2], UV-vis spectroscopy [3], chemiluminescence [4], electrochemiluminescence [5], localized surface plasmon resonance (LSPR) [6] and inductively coupled plasma mass spectrometry (ICP-MS) [7] etc. However, these reported methods often rely on larger and expensive instruments, time-consuming sample pre-treatment process and skilled operators etc. The shortcomings of these methods have limited their practical application in Pb^{2+} detection to a certain extent, and it has been difficult to meet the needs of environmental and food safety monitoring. Therefore, it is necessary to establish a convenient and fast detection technology for Pb^{2+}.[8]

Artificial synthetic functional nucleic acids (FNAs) are nucleic acids that bind to a specific target analyte with specific recognition or have a certain catalytic function, such as ribosome [9], deoxyribozyme (DNAzyme) [10], and aptamer [11]. After nearly 30 years of efforts by analysts worldwide, FNAs have been widely used in biosensors due to the advantages of low cost, high affinity, high sensitivity, excellent stability and flexible design. The recognition units in FNAs based Pb^{2+} biosensors are mainly GR-5′-deoxyribozyme[12], 8-17E deoxyribozyme [13] and aptamer [14]. Compared to the RNA-cleaving deoxyribozymes, aptamer based Pb^{2+} biosensors are increasing popular because of simple operation, flexible design and low detection cost. As a pioneering work, Wang et al. developed a label-free, fluorescence turn-on biosensor for Pb^{2+} based on conformation switch of Pb^{2+} aptamer T30695 and PPIX as fluorescence read out with the limit of detection (LOD) of 20 nM. [15] PPIX is a water-soluble, weakly fluorescent cationic porphyrin but emit strong fluorescence when it specifically binds to the parallel G-quadruplex (G4). The background fluorescence from the free dye in the solution limits the further improvement of the sensitivity of the label-free biosensors. At the same time, higher concentration of Pb^{2+} could quench the fluorescence of PPIX which may due to the fact that Pb^{2+} is a fluorescence quenching agent. [16] Yu et al. reported Na^+ could further improve the binding efficiency of Pb^{2+}-stabilized T30695 with the ZnPPIX and proposed a fluorescent Pb^{2+} biosensor using the Na^+-induced conformational switch of Pb^{2+}-stabilized T30695 G4. [17] Accordingly, the sensitivity was improved with the LOD of 10 nM. Yang et al. designed a logic gate platform for simultaneously detection of Pb^{2+} (LOD = 15 nM) and Ag^+ (LOD = 191 nM) based on the target induced G-rich Pb^{2+} aptamer and C-rich i-motif structure switch and the various assembly states of fluorescent cyanine dye as the readout. [18] Very recently, Qiu and liu *et al.*

[a.] *National Engineering Research Center of Coal Preparation and Purification; Key Laboratory of Coal Processing and Effcient Utilization of Ministry of Education, School of Chemical Engineering and Technology, China University of Mining & Technology, Xuzhou, 221116, China. Email: 8422127@alu.fudan.edu.cn*
[b.] *Henan Key Laboratory of Biomolecular Recognition and Sensing, College of Chemistry and Chemical Engineering, Henan Joint International Research Laboratory of Chemo/Biosensing and Early Diagnosis of Major Diseases, Shangqiu Normal University, Shangqiu, 476000, China. Email:xumaotian@sqnu.edu.cn*
[c.] *College of Chemistry and Chemical Engineering, Xinjiang Normal University, Urumqi, 830054, China.*
† These authors contributed equally to this work.
Electronic Supplementary Information (ESI) available. See DOI: 10.1039/x0xx00000x

View Article Online
DOI: 10.1039/D0CC03669B

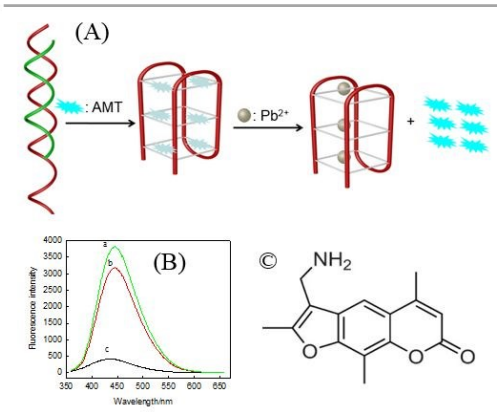

Fig. 1 (A) Schematic representation of the proposed fluorescent Pb^{2+} biosensor utilizing binding induced quenching of AMT to G-quadruplex. (B) Fluorescent spectra of AMT at 4 μM (curve a) in the presence of different chemical species of T30695 (curve c) and coexisting of T30695, Z and Pb^{2+} (curve b) in 10 mM MES-Tris buffer (pH 5.0). λex= 340 nm. (C) Chemical structure of AMT.

reported the metalation activity of T30695 was significantly accelerated by Pb^{2+} and suggested a fluorescent ratiometric Pb^{2+} biosensor based on the efficient DNA-catalyzed porphyrin metalation with the LOD of 23.5 nM. [19] All of the developed Pb^{2+} biosensors exhibit reliable, specific and sensitive detection of target in clinically relevant complex samples, such as serum, urine and even living cells. Applications of aptamer to Pb^{2+} detection with improved sensitivity remain to be explored. Herein, we reported a novel aptamer based fluorescent Pb^{2+} biosensor with improved sensitivity using the binding induced quenching of fluorophore to T30695 aptamer, as shown in Fig. 1A. AMT (chemical structure was given in Fig. 1C) is chosen as a fluorescent indicator because this dye emits strong fluorescence in solution (Fig. 1B, curve *a* in green). The fluorescence of AMT could be quenched once binds to G4 (lg*K*=5) in 1:1 ratio via end-stacking mode to form the G4/AMT complex, which seems to result from the electron transfer from the guanine moiety of G4 to photo excited AMT.[20] At the same time, double strand DNA has no effect on AMT fluorescence.[20] T30695 is employed as the recognition unit as its specific binding with Pb^{2+} (lg*K* = 7) and folded into G4.[15] The addition of T30695 to the AMT solution essentially quenched the fluorescence of AMT (Fig. 1B, curve *c* in black) which is consistent with the recent report.[20] Thus, we infer that AMT could be acted as an excellent readout dye by virtue of the binding induced effectively quenching and be released from the G4/AMT complex through competitive binding of Pb^{2+}, and the emission was restored. However, the further addition of Pb^{2+} to the solution containing T30695/AMT complexes, the fluorescence change was negligible (data not shown). The results clearly suggested that the difference of affinity between T30695 and AMT or Pb^{2+} was too weak to displace AMT from T30695/AMT complexes by Pb^{2+}. So, six DNA sequences that could bind to Pb^{2+} were examined (Fig. S1 in supporting information). However, the sensing performance was not as expected. This may be due to the difference of the affinity of G4 for AMT and Pb^{2+} is not enough. To work the designed sensor, an intermediate was needed to reduce the affinity of T30695/AMT complexes or replace AMT from T30695/AMT complexes through the synergistic interaction

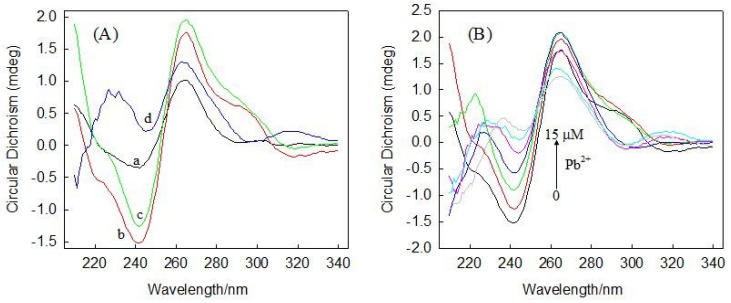

Fig. 2 CD spectra of (A) 0.2 μM T30695, 0.2 μM T30695+Z, 0.2 μM T30695+Z+AMT (4 μM) and T30695+Z+AMT (4 μM)+Pb^{2+} (5 μM) in 10 mM MES-Tris buffer (pH 5.0). (B) The sensing system upon addition of different amounts of Pb^{2+} (0, 1, 3, 5, 10, 15, 20 μM) in 10 mM MES-Tris buffer (pH 5.0). The arrow indicates the change in signal observed as the Pb^{2+} concentration increases.

with Pb^{2+} or both. According to the literature[15], several DNA strands with different base numbers complementary to T30695 was optimized (Fig. S1 in supporting information). As a result, when Pb^{2+} was added to the solution coexisting of T30695, Z and AMT, the fluorescence intensity of the system was significantly enhanced (Fig. 1B, curve *b* in red). As a control test, Pb^{2+} could not induce remarkable variations in the AMT fluorescence spectra (data not shown). To the best of our knowledge, there is no report of the aptamer T30695 based fluorescent Pb^{2+} biosensors using the intrinsic quenching ability of G4. This study not only provides a novel fluorescent Pb^{2+} biosensor but also paves an avenue to the development of new fluorescent methods based on the rational design. [21] The conformational changes of the used DNA sequences in this work were characterized by circular dichroism (CD) spectroscopy. As shown in Fig. 2A (curve *a*), a strong positive peak at 265 nm and a negative peak at 240 nm were observed, indicating that parallel conformation was the predominant. When T30695 and Z hybridize, a strong positive CD peak at 285 nm and a negative CD peak at 255 nm were observed, indicating that B-form DNA was the predominant conformation (Fig. 2A, curve *b*).[22] No significant change was seen in the CD spectrum of the system when further addition of AMT to the duplex solution, indicating that AMT does not cause conformational changes of duplex DNA (Fig. 2A, curve *c*). The addition of Pb^{2+} to the sensing system induces an enhancement in the positive band and the shoulder was disappeared (Fig. 2A, curve *d*). Additionally, a small but clean positive peak near 310 nm was obtained, which is the typical CD characteristic of the Pb^{2+}-stabilized antiparallel G4 structure. [15] In order to further confirm the mechanism of the sensing system, CD spectra were recorded in the presence of different concentrations of Pb^{2+} from 1 μM to 20 μM (Fig. 2B). As can be seen from Fig. 2B, both the positive peak at 265 nm and the negative peak at 240 nm were decreased and the small positive peak at 310 nm was increased. This CD spectrum

suggests the coexistence of the parallel G4 structures with a small amount of the antiparallel ones. [23]

Experimental conditions were optimized including incubation time (Fig. S2), the effect of K^+ amount (Fig. S3), pH (Fig. S4), the ratio of T30695 and Z (Fig. S5), DNA concentration (Fig. S6) and AMT concentration (Fig. S7) and the results are given in supporting information.With the aim of developing a reliable analytical method for detecting Pb^{2+} in a real biological complex sample, we investigated the selectivity of the developed T30695 aptamer/AMT complex based biosensor using the common metal ions such as K^+, Ca^{2+}, Na^+, Mg^{2+}, Al^{3+}, Zn^{2+}, Fe^{3+}, Cu^{2+}, Hg^{2+}, Ag^+, Cr^{3+}, Ni^{2+}, Mn^{2+}, Cd^{2+}, and the mixture of these ions at the same concentration of Pb^{2+}, and the results are given in Fig. 3A. The results show that metal ions other than Pb^{2+} could not enhance any detectable fluorescence and thus have little or even no interference for Pb^{2+} detection. To confirm the selectivity of the proposed sensing system, the competition tests were also performed by introducing of Pb^{2+} in the presence of the interfering salts, and the results are given in Fig. 3B. The two red columns are both performed in the presence of Pb^{2+}. The lower one is in the presence of only Pb^{2+}, and the slighter higher one is in the presence of Pb^{2+} and other metal

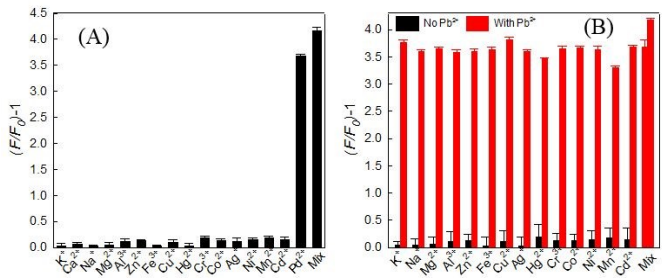

Fig. 3 Selectivity of the proposed sensing system. (A) Histogram of fluorescent intensity in the presence of Pb^{2+} and other interfering ions at the 5.0 μM levels and the mixture of aforementioned metal ions in 10 mM MES-Tris buffer (pH 5.0) and (B) The responds of the sensing system to Pb^{2+} (5.0 μM) in the presence of possible competitors at the same amount and a mixture containing all of the tested substances in 10 mM MES-Tris buffer (pH 5.0). The error bars represent the standard deviations and were based on three replicate measurements.

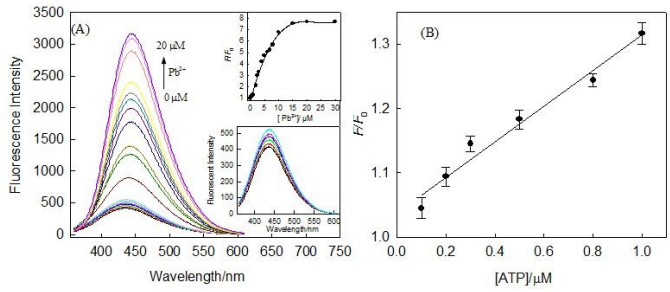

Fig. 4 Fluorescent spectra of the proposed sensing system in the presence of different amount of Pb^{2+} (from top to bottom is from bottom to top: 0.1, 0.2, 0.3, 0.5, 0.8, 1.0, 2.0, 2.5, 3.0, 4.0, 5.0, 6.0, 7.0, 8.0, 10.0, 15.0, 20.0 μM) in 10 mM MES-Tris buffer (pH 5.0) containing 4 μM AMT and 4 μM DNA. The inset shows the evolution of maximum fluorescent intensity vs the concentration of Pb^{2+}. λex=340 nm. (B) Linear plot of the relative fluorescence intensity (F/F_0) as a function of the increasing concentrations of Pb^{2+}. F and F_0 were the maximum fluorescence intensity of the developed sensing system in the presence and the absence of Pb^{2+}, respectively.

ions. The results show that other metal ions do not interfere with the Pb^{2+} detection too. Both the experiments confirmed the high selectivity of the sensor for Pb^{2+}. Such an outstanding specificity of the T30695 aptamer/AMT complex based biosensor for Pb^{2+} may be attributed to the fact that Pb^{2+} has a much stronger affinity toward the T30695 aptamer, which would effectively avoid false positives.

After examined the selectivity, we monitored the fluorescence emission spectra of our developed biosensor in the MES-Tris buffer containing various amounts of Pb^{2+} under these optimized experimental conditions (Fig. 4A). It was found that the aptamer T30695/AMT complex is weakly emissive in MES-Tris buffer before Pb^{2+} addition. However, significant enhancement step by step in emission around 450 nm was observed upon the addition of Pb^{2+} from 10 nM to 10 μM into the sensing system. The fluorescence enhancement (F/F_0) versus the amount of Pb^{2+} was also plotted. Here, F and F_0 represent the fluorescence intensity with and without Pb^{2+} (Fig. 4A, inset). When the Pb^{2+} concentrations were above 10 μM, the fluorescence signal (F/F_0) reaches to the maximum about 8 times. At the same time, the calibration curve is achieved by plotting the fluorescence enhancement (F/F_0) versus Pb^{2+} concentrations from 0.1 μM to 1.0 μM (Fig. 4B). The fitting equation could be expressed as y=0.2763x+1.0378 with linear correlation coefficient r = 0.987. The LOD was calculated to be 3.6 nM according to the IUPAC definition ($3\sigma/K$ rules), where σ is the standard deviation of 10 blank solutions and K is the slope of the calibration curve. Fig. S8 in Supporting Information shows the working curve at high concentrations. Table S2 in Supporting Information compares the sensing performances of the present biosensor with some reported methods for Pb^{2+} determinations. In comparison with other reported methods, our suggested biosensor here is more sensitive than most of the reported sensors. Such a high sensitivity maybe originates from the insignificant background fluorescence with the turn-on readout, which would effectively avoid false negatives.

By use of the present biosensor, the quantitative measurement of Pb^{2+} in spiked human serum was achieved which suggest our novel biosensor holds a great feasible promise in practical application. The fluorescence emission spectra of our developed biosensor in the presence of various amounts of Pb^{2+} in spiked human serum were given in Fig. S9A (Supporting Information). The signal F/F_0 versus the amount of Pb^{2+} was also plotted (Fig. S9B, Supporting Information). With the developed calibration plot, the concentrations of Pb^{2+} were quantitatively determined using the obtained calibration curve and the accuracy of the present method was evaluated by recovery and the results were tabulated in Table S3 in Supporting Information. The recoveries are between 95% and 110%, which indicates the high accuracy of the present method. The results were further validated by ICP-AES (Table S3 in Supporting Information). These results indicate that the

present biosensor could be successfully applied to detect Pb^{2+} in real clinical samples.

In summary, a novel T30695 aptamer/AMT complex based biosensor has been suggested and evaluated for quantitative detection of Pb^{2+} in human serum with high sensitivity and specificity. The T30695 aptamer/AMT complex is weakly fluorescent in solution in the absence of Pb^{2+}, while highly fluorescent upon the binding of T30695 to Pb^{2+} and subsequently displacement of AMT from the T30695 aptamer/AMT complex. The validity of practical application of the developed biosensor was demonstrated by successful quantitative detecting Pb^{2+} in real clinical complex samples. Moreover, more biosensors for biological determination and clinical analysis could be designed by changing T30695 to other target-specific G4 aptamers combining with the signal amplification technologies.

The authors acknowledge the financial support from the National Natural Science Foundation of China (Grant nos. 21575087, 51574237), Xuzhou Science and Technology Plan Project (KC19228), Innovation Scientists and Technicians Troop Construction Projects of Henan Province (No: 41).

Conflicts of interest

There are no conflicts to declare.

Notes and references

1 Yang. D, Liu. X, Zhou. Y, Luo. L, Zhang. J, Huang. A, Mao. Q, Chen. X and Tang. L, *Anal. Methods*, 2017, **9**, 1976.

2 Tahán. J. E., Granadillo. V. A. and Romero, R. A., *Anal. Chim. Acta.,* 1994, **295**, 187; Badiei. H. R., Liu. C. and Karanassios. V., *Microchem J.*, 2013, **108**, 131.

3 Qiu. J., Li. Z., Miao. L., Wang. H., Zhang. Y., Wu. S., Zhang. Y., Li. X. and Wu. A., *Analyst*, 2019, **144**, 5081; Wang. D., Ge. C., Lv. K., Zou. Q., Liu. Q., Liu. L., Yang. Q. and Bao. S., *Chem. Commun.* 2018, **54**, 13718-13721.

4 Wang. H., Wang. D. M. and Huang. C. Z., *Analyst*, 2015, **140**, 5742.

5 Lei. Y.-M., Huang. W.-X., Zhao. M., Chai. Y.-Q., Yuan. R. and Zhuo Y., *Anal. Chem*., 2015, *87*, 7787.

6 Qiu. G., Ng. S. P., Liang. X., Ding. N., Chen. X. and Wu. C.-M. L., *Anal. Chem.*, 2017, **89**, 1985.

7 Li. P.-C. and Jiang. S.-J., *Anal. Bioanal. Chem.*, 2006, **385**, 1092.

8 Wang. G., Chu. L. T., Hartanto. H., Utomo. W. B., Pravasta. R. A. and Chen. T.-H., *ACS Sensors*, 2020, **5**, 19.

9 Famulok. M., Hartig. J. S. and Mayer G., *Chem. Rev.*, 2007. **107**, 3715.

10 Liu. J., Cao. Z. and Lu. Y., *Chem. Rev.*, 2009, **109**, 1948.

11 McConnell. E. M., Cozma. I., Morrison. D. and Li. Y., *Anal. Chem.*, 2020, **92**, 327.

12 Huang. Y., Lin. C., Luo. F., Qiu. B., Guo. L., Lin. Z. and Chen. G., *ACS Sensors*, 2019, **4**, 2465; Ji. R., Niu. W., Chen. S., Xu. W., Ji. X., Yuan. L., Zhao. H., Geng. M., Qiu. J. and Li C., *Biosen. Bioelectron.*, 2019, **144**, 111560.

13 Ravikumar. A., Panneerselvam. P., Radhakrishnan. K., Morad. N., Anuradha. C. D. and Sivanesan, S., *J. Fluoresc.*, 2017, **27**, 2101; Xiang. Y., Tong. A., Lu. Y., *J. Am. Chem. Soc.*, 2009,**131**, 15352.

14 Fakhri. N., Hosseini. M. and Tavakoli. O., *Anal. Methods*, 2018, **10**, 4438; Li. C. N., Fan. P. D., Liang. A. H., Liu. Q. Y. and Jiang. Z. L., *Microchim. Acta.*, 2018,**185**, 8; Taghdisi. S. M., Danesh. N. M., Lavaee. P., Ramezani. M. and Abnous. K., *Sens. Actuator B-Chem.*, 2016, **234**, 462.

15 Li. T., Dong. S. and Wang. E., *J. Am. Chem. Soc.*, 2010, **132**, 13156.

16 Chen. J., Liu. J., Fang. Z. and Zeng. L., *Chem. Commun.*, 2012, **48**, 1057; Wang. H. B., Ma. L. H., Fang. B. Y., Tan. F., Cao. Y. C., Zhao. Y. D. and Hu. X. B., *Sens. Actuator B-Chem.*, 2018, **261**, 307; Zhang. D., Zhu. M., Zhao. L., Zhang. J., Wang. K., Qi. D., Zhou. Y., Bian. Y. and Jiang. J., *Inorg. Chem.*, 2017, **56**, 14533.

17 Yu. Z., Zhou. W., Han. J., Li. Y., Fan. L. and Li. X., *Anal. Chem.*, 2016, **88**, 9375.

18 Yang. C., Yang. S., Li. J., Du. Y., Song. L., Huang. D., Chen. J., Zhou. Q., Yang. Q. and Tang. Y., *Anal. Chem.*, 2018, **90**, 10585.

19 Peng. D., Li. Y., Huang. Z., Liang. R.-P., Qiu. J.-D. and Liu. J., *Anal. Chem.*, 2019, **91**, 11403.

20 Paul. S. and Samanta. A., *J. Phy. Chem. B.*, 2018, **122**, 2277.

21 Deng. J., Jiang. Q., Wang. Y., Yang. L., Yu. P. and Mao. L., *Anal. Chem.*, 2013, **85**, 9409.

22 Yu. H.-Q., Miyoshi. D. and Sugimoto. N., *J. Am. Chem. Soc.*, 2006, **128**, 15461.

23 Kypr. J., Kejnovská. I., Renčiuk. D. and Vorlíčková, M., *Nucleic Acids Res.*, 2009, **37**, 1713; Mergny. J.-L., Li. J., Lacroix. L., Amrane. S. and Chaires. J. B., *Nucleic Acids Res.*, 2005, **33**, e138-e138.

View Article Online
DOI: 10.1039/D0CC03669B

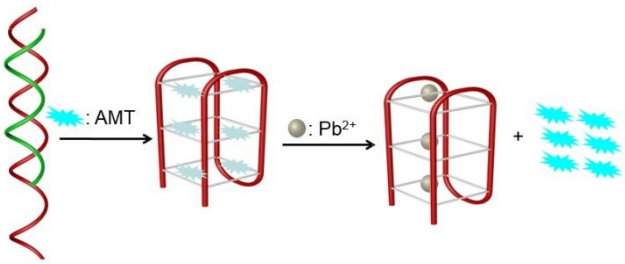

Binding induced quenching of AMT to G-quadruplex was first used to design improved fluorescent Pb^{2+} aptasensor.